Physiological roles of endocytosis and presynaptic scaffold in vesicle replenishment at fast-signaling and slow-plastic synapses

Satyajit Mahapatra [a, 1] and Tomoyuki Takahashi [a, 1]

[a] Cellular and Molecular Synaptic Function Unit, Okinawa Institute of Science and Technology Graduate University (OIST), Okinawa 904-0495, Japan

[1]To whom correspondence may be addressed: satyajit.mahapatra@oist.jp (S.M.), ttakahas@oist.jp (T.T.)

S.M. and T.T. designed research; S.M. performed research; S.M. and T.T. wrote the paper.

The authors declare no competing interest.

Abstract

After exocytosis, release sites are cleared of vesicular residues to be replenished with transmitter-filled vesicles. Endocytic and scaffold proteins are thought to underlie this mechanism. However, physiological significance of the site-clearance mechanism among diverse central synapses remains unknown. Here, we tested this using action-potential evoked EPSCs at fast-signaling calyx and slow-plastic hippocampal CA1 synapses in post-hearing mice brain slices at physiological temperature and Ca^{2+}. Pharmacological block of endocytosis enhanced synaptic depression at the calyx synapse, whereas it attenuated synaptic facilitation at the hippocampal synapse. Block of scaffold protein activity likewise enhanced synaptic depression at the calyx but had no effect at the hippocampal synapse. At the calyx, enhancement of synaptic depression by blocking endocytosis or scaffold activity occurred at nearly identical time courses with a time constant of several milliseconds starting immediately after the stimulation

onset. Neither endocytic nor scaffold protein inhibitors prolonged the recovery from short-term depression. We conclude that endocytic release-site clearance can be a universal phenomenon supporting vesicle replenishment across fast-signaling and slow-plastic synapses, whereas presynaptic scaffold mechanism likely plays a specialized role in vesicle replenishment predominantly at fast synapses.

Keywords*:*

Endocytosis, vesicle replenishment, scaffold protein, release site-clearance, physiological condition, calyx of Held, hippocampal SC-CA1 synapse, synaptic depression, synaptic facilitation.

Introduction

Chemical synaptic transmission depends upon fusion of transmitter-filled vesicles with the presynaptic membrane. At presynaptic terminals, there are a limited number of vesicular release sites, which can become refractory while discharged vesicles are remaining at the site (Katz, 1993), inhibiting subsequent vesicle fusion. Following inactivation of the temperature-sensitive endocytic protein dynamin in *Drosophila* mutant *Shibire*, short-term depression (STD) of neuromuscular transmission is enhanced within tens of milliseconds of the onset of stimulation (Kawasaki et al., 2000), suggesting that vesicular endocytosis plays a significant role in release site-clearance, in addition to its well-established role in the vesicle recycling (Neher and Sakaba, 2008). At the calyx of Held, in slices from pre-hearing rats, pharmacological block of endocytosis slightly enhances STD and markedly prolongs the recovery from STD (Hosoi et al., 2009). Likewise, at cultured hippocampal synapses, blocking endocytosis

enhances depression at high-frequency stimulation due to slow clearance of vesicular component from release-sites (Hua et al., 2013). Genetic ablation of the endocytic adaptor protein AP-2μ (Jung et al., 2015), synaptophysin (Rajappa et al., 2016), or the secretory carrier membrane protein SCAMP5 (Park et al., 2018) enhances synaptic depression in cultured cells, in agreement with the site-clearance role of endocytosis.

The presynaptic scaffold protein intersectin is a guanine nucleotide exchange factor, which activates the Rho-GTPase CDC42, thereby regulating the filamentous (F) actin assembly (Hussain et al., 2001; Marie et al., 2004). At the calyx of Held in slices from pre-hearing rodents, genetic ablation of intersectin 1 or pharmacological block of CDC42 abolishes the fast component of the rate of recovery from STD (Sakaba et al., 2013), suggesting that the scaffold protein cascade, comprising intersectin, CDC42 and F-actin, contributes to rapid vesicle replenishments possibly through release site-clearance (Japel et al., 2020).

Although the site-clearance hypothesis is well supported, its physiological significance among diverse central synapses remains unknown. To address this, we evoked EPSCs by afferent fiber stimulations in post-hearing (P13-15) mice brain slices, without intra-terminal perturbation, at brainstem calyces of Held and at hippocampal CA1 synapses at physiological temperature (PT, 37°C; Sanchez-Alavej et al., 2011) and in artificial cerebrospinal fluid (aCSF) containing 1.3 mM-Ca^{2+}, in reference to rodent CSF (Jones and Keep, 1988; Silver and Erecinska, 1990; Inglebert et al., 2020). The post-hearing calyx of Held is a fast-signaling relay synapse that can respond to inputs up to 500 Hz without failure *in vivo* (Sonntag et al., 2009) and displays short-term depression during repetitive stimulation. In contrast, the hippocampal CA1 synapse is a relatively slow synapse that starts to fail transmission from Schaffer collateral (SC) to

CA1 pyramidal cells (PC) at 40 Hz in slice (Combe et al., 2018) and exhibits short-term facilitation and long-term plasticity. At these different synapses, we tested the effect of blocking endocytosis or scaffold protein cascade activity on EPSCs evoked by a train of repetitive stimulations (30x) at different frequencies. These experiments indicated that the endocytosis-driven site-clearance mechanism activity-dependently supports vesicle replenishment, thereby counteracting synaptic depression at brainstem calyceal synapses and boosting synaptic facilitation at hippocampal SC-CA1 synapses. In contrast, the vesicle replenishing role of the scaffold mechanism is independent of activity and restricted to fast calyceal synapses, where it co-operates with the endocytosis-dependent site-clearance, thereby maintaining synaptic strength and enabling high-fidelity fast neurotransmission.

Results

Potency of endocytic blockers on slow and fast endocytosis at the calyx of Held

To clarify physiological roles of endocytosis in high-frequency synaptic transmission, we first examined the effect of different endocytic inhibitors on fast and slow endocytosis, using presynaptic membrane capacitance measurements (Sun et al., 2004; Yamashita et al., 2010) at post-hearing calyces of Held (P13-15) at PT (37°C; Renden and von Gersdorff 2007) in aCSF containing 2.0 mM [Ca^{2+}] (Figure 1) to ensure sufficient Ca^{2+}currents to induce exo-endocytosis. Dynasore is a dynamin-dependent endocytosis blocker (Macia et al., 2006; Newton et al., 2006) blocking both clathrin-mediated and clathrin-independent endocytosis (Park et al., 2013; Delvendahl et al., 2016). A second endocytosis blocker Pitstop-2 is thought to preferentially block clathrin-mediated endocytosis (von Kleist et al., 2011; Delvendahl et al., 2016; Lopez-

Hernandez et al., 2022) but it reportedly blocks clathrin-independent endocytosis as well (Dutta et al., 2012; Willox et al., 2014). Since genetic ablation of endocytic proteins can be associated with robust compensatory effects (Ferguson et al., 2009; Park et al., 2013), we adopted acute pharmacological block using endocytic inhibitors Dynasore and Pitstop-2.

At calyces of Held, a single short (5 ms) command pulse elicited an exocytic capacitance jump (ΔC_m) followed by a slow endocytic decay rate (29 fF/s, Figure 1A). In the presence of Dynasore (100 μM) or Pitstop-2 (25 μM) in the perfusate (within 10-60 min of application) this slow endocytosis showed a strongly prolonged time course without accompanied by the change of ΔC_m or presynaptic Ca^{2+} currents (Table S1). In a repetitive stimulation protocol, the accelerating endocytosis can be induced by a 1-Hz train of 20-ms square pulses (Wu et al., 2005; Yamashita et al., 2010). Dynasore or Pitstop-2 significantly inhibited the maximal rate of 250 fF/s of this accelerated fast endocytosis (20 ms x 15 times at 1 Hz) to ~ 50 % (Figure 1B, Table S1). In another stimulation protocol (Figure 1C), 10 command pulses (20 ms duration) applied at 10 Hz induced a fast endocytosis with a decay rate (350 fF/s) by more than 10 times faster than the slow endocytosis elicited by a 5 ms pulse (Figure 1A). Dynasore or Pitstop-2 significantly inhibited the rate of this fast endocytosis (Figure 1C, Table S1) too. The potencies of bath-applied Dynasore or Pitstop-2 for blocking slow and fast forms of endocytosis were comparable to that of dynamin-1 proline-rich domain peptide (Dyn-1 PRD peptide) directly loaded in calyceal terminals (1mM; Figure S1; Yamashita et al., 2005). Thus, at calyces of Held, bath-application of Dynasore or Pitstop-2 can block both fast and slow endocytosis without perturbing presynaptic intracellular milieu.

Effects of endocytic blockers on synaptic depression and recovery from depression at brainstem calyceal synapses

Using Dynasore or Pitstop-2, we investigated the effect of blocking endocytosis on synaptic transmission at the calyx of Held in brainstem slices from post-hearing mice (P13-15). At PT (37°) in physiological aCSF (1.3mM [Ca^{2+}]), EPSCs were evoked by a train of 30 stimulations applied to afferent fibers at 10 or 100 Hz (Figure 2). Neither Dynasore nor Pitstop-2 (in the perfusate, within 10-60 min of application) affected the first EPSC amplitude in the train (Figure S2A). During a train of stimulations at 10 Hz, in the presence of Dynasore (100 μM), synaptic depression was slightly enhanced (from 45% to 52%, by 1.15 times), whereas Pitstop-2 had no effect (Figure 2A1). At 100-Hz stimulations, however, both Dynasore and Pitstop-2 markedly and equally enhanced synaptic depression within 10 ms from the stimulus onset, increasing the magnitude of steady state STD (averaged from #26-30 EPSCs) from 58% to 75% (1.3 times; $p < 0.001$, t-test; Figure 2B1). These results suggest that endocytosis-dependent rapid SV replenishment operates during high-frequency transmission at the mammalian central synapses like at the neuromuscular junction (NMJ) of *Drosophila* (Kawasaki et al., 2000). Since glutamate released during action potential evoked EPSCs does not desensitize or saturate postsynaptic receptors at post-hearing calyces of Held (Ishikawa et al, 2002) unlike at pre-hearing calyces (Yamashita et al, 2009), enhanced synaptic depression in the presence of endocytic blockers during repetitive fiber stimulations is most likely caused by pre-synaptic mechanisms. In fact, the results of endocytic block were essentially the same in the absence (Figure 2) or presence (Figure 3S) of the low-affinity glutamate receptor ligand kynurenic acid (1 mM), which reduces postsynaptic receptor occupancy with glutamate.

At pre-hearing calyces of Held at room temperature (RT), in 2.0 mM [Ca^{2+}] solution, with a long command pulse stimulation under voltage-clamp, dynamin inhibitors markedly prolong the recovery of EPSCs from STD (Hosoi et al., 2009). In contrast, at post-hearing calyces in 1.3 mM [Ca^{2+}] and at PT (37°C), in the presence of the endocytic blockers, recovery of EPSCs from STD showed no prolongation (Figure 2A2, 2B2, Table S2). Conversely, the recovery from STD caused by 100-Hz stimulation was significantly accelerated at both fast and slow recovery time constants (Figure 2B2, Table S2). To explore the reason for these different results, we raised Ca^{2+} concentration in aCSF to 2.0 mM at PT (Figure S4A) or RT (Figure S4B) or raised stimulation frequency to 200 Hz at PT (Figure S4C). None of these manipulations caused significant change in the recovery from STD (Figure S4). Remaining difference may include the species and age differences between animals (pre-hearing rats *vs* post-hearing mice) and stimulation intensity that is stronger in the whole-cell voltage-clamp command pulse protocol than afferent fiber stimulation. Lack of recovery acceleration in 2.0 mM [Ca^{2+}] (Figure S4) by Dynasore or Pitstop-2 is consistent with the observation in dynamin-1 knockout mice (Mahapatra et al, 2016) suggesting that recovery acceleration of unknown mechanism observed in physiological [Ca^{2+}] and temperature (Figure 2B2) was likely masked in 2.0 mM [Ca^{2+}].

Effects of scaffold protein cascade inhibitors on vesicle endocytosis, synaptic depression, and recovery from depression at brainstem calyceal synapses

Among presynaptic scaffold proteins, F-actin is assembled by the Rho-GTPase CDC42 activated by the scaffold protein intersectin, a guanine nucleotide exchange factor (Hussain et al., 2001; Marie et al., 2004). Genetic ablation of intersectin 1 or

pharmacological inhibition of CDC42 activity prolongs the recovery from STD at pre-hearing calyces of Held, suggesting that this scaffold cascade contributes to vesicle replenishment, possibly via release site-clearance (Sakaba et al., 2013; Japel et al.,2020).

Genetic ablation of intersectin inhibits endocytosis in cultured synapses (Yu et al., 2008), but does not affect endocytosis at pre-hearing calyces of Held (Sakaba et al., 2013). We examined the effect of blocking CDC42 using ML 141 (10 μM, 10-60 min) or inhibiting F-actin assembly using Latrunculin-B (15 μM, 10-60 min) in perfusates on fast and slow endocytosis at the post-hearing (P13-15) calyx of Held at PT (Figure 3) in aCSF containing 2.0 mM [Ca^{2+}]. In agreement with previous report (Sakaba et al., 2013), none of these inhibitors affected the fast or slow forms of endocytosis.

We then recorded EPSCs in 1.3 mM [Ca^{2+}] at PT. Neither ML141 nor Latrunculin-B affected the first EPSC amplitude in the train (Figure S2A), alike Latrunculin-B effects at RT and 2.0 mM [Ca^{2+}] (Mahapatra et al., 2016; Mahapatra and Lou. 2017). During a train of stimulations at 10 Hz (Figure 4A1) or 100 Hz (Figure 4B1), in the presence of ML141 or Latrunculin-B in perfusates, synaptic depression was markedly and equally enhanced, with STD magnitude (#26-30) increasing from 45% to 62% (1.4 times; $p < 0.001$, t-test; Figure 4A1) at 10 Hz and from 58% to 80% at 100 Hz (1.4 times; $p < 0.001$, t-test; Figure 4B1). Thus, in contrast to endocytic blockers (Figure 2), the depression-enhancing effects of scaffold cascade inhibitors were not activity-dependent.

Like endocytic blockers, scaffold cascade inhibitors did not prolong the recovery from STD at 10 Hz (Figure 4A2) or at 100 Hz (Figure 4B2). These results contrast with those previously reported at pre-hearing calyces (Sakaba et a, 2013), where genetic ablation of intersectin or pharmacological block of CDC42 prolongs the recovery from

STD induced by double command pulse stimulation under voltage-clamp.

Kinetic comparison of synaptic depression enhanced by endocytic blockers and scaffold cascade inhibitors and evaluation of their combined effect

During 100-Hz stimulation, enhancement of synaptic depression by endocytic blockers or scaffold cascade inhibitors are prominent already in the second EPSCs (Figure 2B1, 4B1). Exponential curve fits to data points (Figure 5A) indicated that the EPSCs underwent a single exponential depression in controls with a mean time constant of 37 ms (n = 11), whereas in the presence of endocytic blockers or scaffold cascade inhibitors, EPSCs amplitude underwent double exponential decay with a fast time constant of 5-10 ms and a slow time constant of tens of milliseconds, the latter of which was similar to the time constant in control (Figure 5B). These data indicate that endocytic and scaffold mechanisms for vesicle replenishment operate predominantly at the beginning of synaptic depression. This is consistent with a lack of prolongation in the recovery from STD by endocytic blockers or scaffold cascade inhibitors (Figure 2A2, 2B2; Figure 4A2, 4B2).

Since the enhancement of synaptic depression by endocytic blockers or scaffold cascade inhibitors occurred mostly at the early phase of synaptic depression, endocytosis- and scaffold-dependent synaptic strengthening likely operate simultaneously during high-frequency transmission. To clarify whether these mechanisms are additive or complementary, we co-applied Dynasore and Latrunculin-B during 100 Hz stimulation (Figure 5C). The magnitude of EPSC depression by the co-application was the same as that by single Latrunculin-B application (Figure 5C), suggesting that endocytosis and scaffold mechanisms complementarily maintain

synaptic strength during high-frequency transmission.

The F-actin depolymerizers Latrunculin A and Latrunculin B are widely utilized to examine presynaptic roles of F-actin. However, the results of STD and recovery can vary according to the application methods and experimental conditions (Figure S5A). At the calyx of Held, in 2.0 mM [Ca^{2+}] aCSF at PT, Latrunculin A perfusion (20 μM, 1h, Figure 5A1) showed a significant enhancement of STD at 100 Hz within 10-60 min of drug application (Figure S5B1, S5D), as previously reported for Latrunculin B perfusion at RT and 200 Hz (Mahapatra et al, 2016). However, 1h preincubation of slices with Latrunculin A (20 μM) followed by perfusion with standard aCSF (~1h, Figure S5A2) had no significant effect on STD induced by a train of 30 stimuli at 100 Hz (Figure S5B2, S5D), as previously reported (Babu et al, 2020). In 1.3 mM [Ca^{2+}] aCSF at PT (Figure 5C), marked STD enhancement was observed by continuous perfusion of Latrunculin B (15 μM, Figure S5C, Figure S5D) or Latrunculin A (20 μM, Figure S5C, Figure S5D). Thus, Latrunculin A (20 μM) and Latrunculin B (15 μM) are equipotent for STD enhancement in these experiments (Figure S5C, S5D).

When the data are compared between 1.3 mM [Ca^{2+}] and 2.0 mM [Ca^{2+}], STD levels after Latrunculin A perfusion are not different ($p > 0.05$, Figure S5D), whereas control STD level in 1.3 mM [Ca^{2+}] (~0.4) was significantly less than 2.0 mM [Ca^{2+}] (~0.3; $p = 0.0036$, t-test; Figure S5D). Thus, physiological 1.3 mM [Ca^{2+}] revealed a robust STD-counteracting function of F-actin.

Regarding the recovery from STD, Ca^{2+}-dependent recovery (CDR) component of tens of ms time constant is produced by strong stimulation at the calyx of Held at RT (Wang and Kaczmarek, 1998) and inhibited by Latrunculin B (Lee et al, 2013). CDR is also observed after STD induced by 100 Hz stimulation at PT and blocked by

Latrunculin A pretreatment (20 μM) in 2 mM [Ca^{2+}] (Babu et al, 2020). However, such Latrunculin-sensitive fast recovery component was absent in 1.3 mM [Ca^{2+}] (Figure 4B2, Table S2). Thus, CDR may operate only when excessive Ca^{2+} enters during massive presynaptic activation.

Possible role of endocytosis and scaffold machineries at hippocampal synapses

Counteraction of synaptic depression by endocytosis or scaffold mechanism is highlighted at fast synapses of large structure such as neuromuscular junction or the calyx of Held. However, it remains open whether these mechanisms are conserved at more conventional bouton-type synapses involved in synaptic plasticity. Hence, we recorded EPSCs from hippocampal SC-CA1 pyramidal neurons evoked at high frequency (10 Hz or 25 Hz) by stimulating Schaffer collaterals (SCs) at PT and in aCSF containing 1.3 mM [Ca^{2+}] (Figure 6). In this physiologically optimized experimental condition, EPSCs underwent a prominent facilitation (Figure 6). In the presence of Dynasore (100 μM, within 10-60 min of application in perfusate), synaptic facilitation was much less than control, which was noticeable within 300 ms (4th stimulation) at 10 Hz stimulation or within 80 ms (3rd stimulation) at 25 Hz stimulation from the onset (Figure 6A, 6B). Unexpectedly, Dynasore significantly enhanced the basal EPSC amplitude (Figure S2B), whereas Pitstop-2 had no such effect (Figure S2B). Although less potent than Dynasore, Pitstop-2 significantly attenuated synaptic facilitation (Figure 6A, 6C). Thus, at hippocampal CA1 synapses, like at fast synapses, endocytosis strengthens synaptic efficacy during high-frequency transmission, thereby boosting short-term synaptic potentiation.

Strikingly, unlike endocytic blockers, neither ML141 nor Latrunculin-B affected the

hippocampal short-term facilitation during stimulations at 10 Hz or 25 Hz (Figure 6C, 6D). Thus, the presynaptic scaffold cascade proteins F-actin or CDC42 unlikely plays a regulatory role on short-term synaptic plasticity at hippocampal synapses. At the CA1 synapse, block of vesicle acidification is reported to enhance synaptic depression at 10-30-Hz stimulation (Ertunc et al., 2007), presumably because of a lack of filled vesicles undergoing rapid vesicle recycling. However, at hippocampal synapses in culture, vesicle acidification block has no effect on the depression of repetitive exocytosis (Hua et al., 2013). To determine whether this enhanced depression in the presence of v-ATPase blockers in brain slices (Ertunc et al., 2007) have any physiological relevance in regulating the synaptic strength during repetitive transmission, we tested the effect of v-ATPase blockers on hippocampal EPSCs. Unlike in 2.0 mM [Ca^{2+}] aCSF at RT (Ertunc et al., 2007), in 1.3-mM [Ca^{2+}] aCSF at PT, EPSCs showed a prominent facilitation (Figure 6, Figure S6), and blocking vesicle acidification with Folimicin (67 nM) or Bafilomycin A1 (5 μM) reduced the basal EPSC amplitudes but had no significant effect on the short-term facilitation (Figure S6). Thus, in physiological conditions, vesicle acidification has no direct effect on the short-term synaptic plasticity at hippocampal CA1 synapses.

Discussion

In acute slices optimized to physiological conditions, blocking endocytosis by bath-application of endocytic blockers enhanced activity-dependent depression of EPSCs evoked by high-frequency stimulation of afferent fibers at brainstem calyceal synapses. The enhancement of depression occurred immediately after the onset of stimulation and proceeded with a several millisecond time constant and then slowly merged into the

control time course. Thus, the depression-counteracting effect of endocytosis was restricted to the early epoch of high-frequency transmission when many vesicles occupy the release sites. As number of vesicles undergoing exocytosis during repetitive stimulation gradually reduces, the site-clearance becomes less demanding.

At the calyx of Held, Dynasore or Pitstop-2 blocked both fast and slow endocytosis (Figure 1). The fast endocytosis is characterized with a rate of ~350 fF/s, which was slowed by endocytic blockers to ~150 fF/s (Figure 1C, Table S1). This reduction of endocytic rate (200 fF/s) corresponds to 2.54 vesicles/ms (1 fF = 12.7 vesicles; Yamashita et al., 2010; 200 fF/s x 12.7 vesicles x 1/1000 ms). Since the mean amplitude of miniature EPSCs, representing a single vesicle response, was ~55 pA in 1.3 mM [Ca^{2+}] at PT (data not shown), endocytic block is estimated to reduce EPSC amplitude by ~1.4 nA in 10 ms (2.54 vesicles/ms x 55 pA x 10 ms x 1/1000 nA). This is close to the EPSC size difference (1.6 nA) after 10 ms at 100-Hz stimulus onset between the absence and presence of endocytic blockers. Therefore, during high-frequency transmission, the site-clearance by fast endocytosis can fully compensate the initial strong depression. However, the rate of slow endocytosis is 10 times slower than fast endocytosis (Figure 1A, Table S1), therefore slow endocytosis unlikely contributes to the millisecond-order site-clearance. However, without slow endocytosis, vesicular membrane remaining after spontaneous exocytosis would accumulate and congest release sites. Thus, slow endocytosis may play a house-keeping role in release site-clearance.

At the calyx of Held, scaffold protein inhibitors significantly enhanced the early phase of synaptic depression like endocytic blockers (Figure 5A, 5B). Unlike endocytic blockers, scaffold protein inhibitors had no effect on endocytosis (Figure 3).

In contrast to the effect of endocytic blockers (Figure 2), the effect of scaffold protein inhibitors was independent of stimulation frequency (Figure 4). Co-application of endocytic and scaffold protein cascade inhibitors revealed that the synaptic strengthening effects of endocytosis and scaffold machinery are complementary rather than additive (Figure 5C). These results together suggest that fast endocytosis quickly clears vesicle residues, whereas scaffold machinery simultaneously replenishes transmitter-filled vesicles to release sites during high frequency transmission (Figure 7). Through this combinatory mechanism synaptic strength and high-fidelity neurotransmission (up to 500 Hz; Sonntag et al., 2009) can be maintained at fast synapses such as the calyx of Held auditory relay synapse.

At hippocampal CA1 synapses the roles of endocytosis and scaffold machineries in fast vesicle replenishment were different from those at the calyx of Held. In slices optimized to physiological condition, short-term plasticity was depressive at calyceal synapses, whereas facilitatory at hippocampal CA1 synapses. Endocytic blockers attenuated synaptic facilitation at this slow-plastic synapse, suggesting that endocytosis is normally boosting synaptic facilitation (Figure 6). Since synaptic strength at facilitatory synapses is determined by a sum of facilitation and depression mechanisms, attenuation of synaptic depression by endocytosis can boost synaptic facilitation. At hippocampal excitatory synapses, short-term facilitation of glutamate release induces long-term potentiation (LTP) of excitatory transmission. Thus, from physiological viewpoints, endocytosis-dependent site clearance can play an essential role in the induction of LTP underlying memory formation.

Strikingly, the scaffold protein inhibitor ML141 or Latrunculin B had no effect on EPSCs at hippocampal CA1 synapses (Figure 6C, 6D). This is surprising since

Latrunculin-A blocks ultra-fast endocytosis in hippocampal culture (Watanabe et al., 2013). Since Latrunculin-B attenuates vesicle docking at parallel fiber-interneuron synapses in cerebellar slices (Miki et al., 2016), presynaptic scaffold machinery likely operates at the cerebellar synapses. The scaffold machinery might play vesicle replenishing role at fast-relay synapses, but not at slow-plastic synapses. In contrast, the site-clearance role of endocytosis seems universal among synapses, irrespective of their transmission speed and plasticity.

Materials and Methods

Animals

All experiments were performed in accordance with the guidelines of the Physiological Society of Japan and animal experiment regulations at Okinawa Institute of Science and Technology Graduate University. C57BL/6J mice of either sex after hearing onset (postnatal day 13-15) were used for the experiment and animals were maintained on a 12-hour light/dark cycle with food and water *ad libitum*

Method Details

Slice preparation (brainstem and hippocampal) and electrophysiology

Following decapitation of C57BL/6J mice under isoflurane anesthesia, brains were isolated and transverse slices (200 μm thick) containing the medial nucleus of the trapezoid body (MNTB) or parasagittal slices (300 μm) containing the hippocampus were cut using a vibratome (VT1200S, Leica) in ice-cold artificial cerebrospinal fluid (aCSF, see below) with reduced Ca^{2+} (0.1 mM) and increased Mg^{2+} (2.9 mM) concentrations and with NaCl replaced by 200 mM sucrose. Slices were incubated for 1h at 37°C in standard aCSF containing (in mM); 115 NaCl, 2.5 KCl, 25 $NaHCO_3$, 1.25

NaH_2PO_4, 1.3 or 2 $CaCl_2$, 1 $MgCl_2$, 10 glucose, 3 myo-inositol, 2 sodium pyruvate, and 0.4 sodium ascorbate (pH 7.3-7.4 when bubbled with 95% O_2 and 5% CO_2, 285-290 mOsm). Unless otherwise noted, EPSCs were recorded in 1.3 mM [Ca^{2+}] aCSF at 37°C. During recording, a brain slice in a temperature-controlled chamber (RC-26GLP, PM-1; Warner instruments) was continuously perfused with aCSF solutions without (control) or with the pharmacological blockers using a peristaltic pump (5-6 µl/s). Recordings with or without the blockers were made from separate cells in different slices from a minimum of 3-4 animals for each set of experiment. In experiments at PT, solutions kept in a water bath (37°C) and passed through an in-line heater (SH-27B, Warner instruments) placed immediately before the recording chamber and maintained at 37°C (± 0.2°C) by a controller (TC-344C, Warner instruments). For RT experiments, no heating was used, and the temperature was within 22-24°C. Recordings in the presence of pharmacological blockers were made within 10-60 min of drug application and for control experiments a slice was kept in the recording chamber no longer than 1 h.

Whole-cell recordings were made using a patch-clamp amplifier (EPC-10 USB, HEKA Elektronik, Germany) from the calyx of Held presynaptic terminals, postsynaptic MNTB principal neurons, or hippocampal CA1 pyramidal neurons visually identified with a 60X water immersion objective (LUMPlanFL, Olympus) attached to an upright microscope (BX51WI, Olympus, Japan). Data were acquired at a sampling rate of 50 kHz using Patchmaster software (for EPC-10 USB) after online filtering at 5 kHz. The patch pipettes were pulled using a vertical puller (PIP6, HEKA) and had a series resistance of 3-4 MΩ.

Membrane capacitance recordings from presynaptic calyx terminal (at PT)

The patch pipettes for presynaptic capacitance recording were wax coated to reduce

stray capacitance and had a series resistance of 6-15 MΩ, which was compensated by up to 60% for its final value to be 6 MΩ. To isolate presynaptic Ca^{2+} currents (I_{Ca}) during membrane capacitance measurements (C_m), tetrodotoxin (1 μM) and tetra-ethyl-ammonium chloride (TEA, 5 mM) were routinely added to block Na^+ and K^+ channels, respectively. Calyx terminals were voltage clamped at a holding potential of -70 mV and a sine wave (peak to peak = 60 mV at 1kHz) was applied. A single pulse (5 ms) or a train of 20 ms pulses (15 stimuli at 1 Hz or 10 stimuli at 10 Hz) to +10 mV were given to induce slow, fast-accelerating, and fast endocytosis. The capacitance trace within 450 ms after the stimulation pulse was excluded from analysis to avoid capacitance artifacts (Yamashita et al., 2005). The exocytic capacitance jump (ΔC_m) in response to a stimulation pulse was measured as difference between baseline and mean C_m at 450-460 ms after the pulse onset. The endocytic rate was measured from the C_m decay phase 0.45-5.45 s from the end of 5 ms stimulation pulse, 0.45-0.95 s for 1 Hz train stimulation and 0.45-1.45 s after the last (10th) pulse for 10 Hz train stimulation. C_m traces were averaged at every 10 ms (for 10 Hz train stimulation) or 20 ms (for 5 ms single or 1 Hz train stimulation).

EPSC recordings from brainstem and hippocampus

For EPSC recordings, brainstem MNTB principal neurons or hippocampal CA1 pyramidal cells were voltage-clamped at the holding potential of -80 mV. To evoke EPSCs a bipolar electrode was placed on afferent fibers between MNTB and midline in brainstem slices or on the Schaffer collateral fibers in the stratum radiatum near the CA1 border in hippocampal slices.

The patch pipettes had a series resistance of 5-15 MΩ (less than 10 MΩ in most cells) that was compensated up to 80% for a final value of ~3 MΩ for EPSC recording from

MNTB neurons. For EPSC recording from hippocampal pyramidal cells, no compensation was made, and capacitance artifacts were manually corrected. Stimulation pulses were applied through an isolator (Model 2100, A-M Systems) controlled by EPC10 amplifier (HEKA).

During EPSC recordings, strychnine-HCl (Sigma, 2 μM), bicuculline-methiodide (Sigma, 10 μM) and D-(-)-2-Amino-5-phosphonopentanoic acid (D-AP5, Tocris, 50 μM) were added to isolate AMPA receptor-mediated EPSCs. In some experiments, to minimize AMPA receptor saturation and desensitization, kynurenic acid (Sigma, 1 mM) was added to aCSF. Unless otherwise specified, the internal pipette solution for presynaptic capacitance measurements contained (in mM): 125 Cs gluconate, 10 HEPES, 20 TEA-Cl, 5 sodium phosphocreatine, 4 Mg-ATP, 0.3 Na-GTP and 0.5 EGTA (pH 7.2-7.3, adjusted with CsOH, adjusted to 305-315 mOsm by varying Cs-gluconate concentration). For EPSC recording, the internal pipette solution contained QX-314 bromide (2 mM) and EGTA, either 5 mM (for MNTB cells) or 0.5 mM (for pyramidal cells), but otherwise identical to the presynaptic pipette solution. Dynasore (100 μM), Pitstop-2 (25 μM), ML 141 (10 μM), Folimycin (also known as Concanamycin A; 67 nM), Latrunculin-A (20 μM), Latrunculin B (15 μM), and Bafilomycin A1 (5 μM) were dissolved in DMSO (final concentration 0.1%, except for Latrunculin-A, 0.2%). Since Latrunculin A, Latrunculin-B and Folimycin are light sensitive, precautions were taken to minimize light exposure during handling and recording. Dynamin 1 proline-rich domain (PRD) peptide (sequence: PQVPSRPNRAP; GenScript) was dissolved in presynaptic pipette solution (1 mM). Membrane capacitance (C_m) recordings in the presence of Dyn-1 PRD peptide were initiated 4-5 min after whole-cell membrane rupture to allow its time of diffusion inside presynaptic terminals.

Data Analysis and Statistics

Experiments were designed as population study using different cells from separate brain slices under control and drug treatment, rather than on a same cell before and after the drug exposure. All data were analyzed using IGOR Pro (WaveMetrics) and Microsoft Excel. All values are given as mean ± SEM and significance of difference was evaluated by Student's unpaired *t*-test, unless otherwise noted. Significance level was set at $p < 0.05$, denoted with asterisks (*$p < 0.05$, **$p < 0.01$, ***$p < 0.001$).

Data and Resources Availability

- All data generated during this study are included in the manuscript.
- Further information about resources should be addressed to authors.

Supplementary Information

Supplementary information includes six figures, two tables and supporting text.

Acknowledgements

We thank Yukiko Goda for comments, Patrick Stoney for editing this paper. This research was supported by funding from Okinawa Institute of Science and Technology to T.T., and Grants-in-Aid for Scientific Research from the Japan Society for the Promotion of Science (21K06445) to S.M.

References

Combe, C. L., Canavier, C. C., and Gasparini, S. 2018. Intrinsic Mechanisms of Frequency Selectivity in the Proximal Dendrites of CA1 Pyramidal Neurons. J Neurosci 38, 8110-8127.

Babu, LPA, Wang, H.Y., Eguchi, K., Guillaud, L., and Takahashi, T. (2020). Microtubule and actin differentially regulate synaptic vesicle cycling to maintain high-frequency neurotransmission. J Neurosci. *40*,131-142.

Delvendahl I, Vyleta NP, von Gersdorf H, Hallermann S. 2016. Fast, temperature-sensitive and clathrin-independent endocytosis at central synapses. Neuron 90, 1-7.

Dutta D, Williamson CD, Cole NB, Donaldson JG. 2012. Pitstop 2 is a potent inhibitor of clathrin-independent endocytosis. PLOS ONE 7, e45799.

Ertunc M, Sara Y, Chung C, Atasoy D, Virmani T, Kavalali ET. 2007. Fast synaptic reuse slows the rat of synaptic depression in the CA1 region of hippocampus. J Neurosci 27, 341-345.

Ferguson, SM, Raimondi A, Paradise S, Shen H, Mesaki K, Ferguson A, Destaing O, Ko G, Takasaki J, Cremona O, et al. 2009. Coordinated actions of actin and BAR proteins upstream of dynamin at endocytic clathrin-coated pits. Dev Cell 17, 811-822.

Hosoi N, Holt M, Sakaba T. 2009. Calcium dependence of exo- and endocytotic coupling at a glutamatergic synapse. 63, 216-229. Neuron 63, 216-229.

Hua Y, Woehler A, Kahms M, Haucke V, Neher E, Klingauf J. 2013. Blocking endocytosis enhances short-term synaptic depression under conditions of normal availability of vesicles. Neuron 80, 343-349.

Hussain N, Jenna S, Glogauer M, Quinn CC, Wasiak S, Guipponi M, Antonarakis SE, Kay BK, Stossel TP, Lamarche-Vaine N, McPherson PS. 2001. Endocytic protein intersectin-1 regulates actin assembly via Cdc42 and N-WASP. Nat Cell Biol 3, 927-932.

Inglebert Y, Aljadeff J, Brunel N, Dominique D. 2020. Synaptic placticity rules with physiological calcium levels. Proc Natl Acad Sci USA 117, 33639-33648.

Ishikawa T, Sahara Y, Takahashi T. 2002. A single packet of transmitter does not saturate postsynaptic glutamate receptors. Neuron 34, 613-621.

Japel M, Gerth F, Sakaba T, Bacetic J, Yao L, Koo S-J, Maritzen T, Freund C, Haucke V. 2020. Intersectin-mediated clearance of SNARE complexes is required for fast neurotransmission. Cell Rep 30, 409-420.

Jones HC, Keep RF. 1988. Brain fluid calcium concentration and response to acute hypercalcemia during development in the rat. J Physiol 402, 579-593.

Jung S, Maritzen T, Wichmann C, Jing Z, Neef A, Revelo NH, Al-Moyed H, Meese S, Wojcik SM, Panou I, Bulut H, Schu P, Ficner R, Reisinger E, Rizzoli SO, Neef J, Strenzke N, Haucke V, Moser T. 2015. Distribution of adaptor protein 2μ (AP-2μ) in cochlear hair cells impairs vesicle reloading of synaptic release sites and hearing. EMBO J 34, 2686-2702.

Katz B. 1993. On neurotransmitter secretion. Interdiscip Sci Rev 18, 359-364.

Kawasaki F, Hazen M, Ordway RW. 2000. Fast synaptic fatigue in *shibire* mutants reveals a rapid requirement for dynamin in synaptic vesicle membrane trafficking, Nat Neurosci 3, 859-860.

Lee JS, Ho, W-K, Neher E, Lee S-H. 2013. Superpriming of synaptic vesicles after their recruitment to the readily releasable pool. Proc Natl Acad Sci USA 110, 15079-15084.

Lopez-Hernandez T, Takenaka K-I, Mori Y, Kongpracha P, Nagamori S, Haucke V, Takamori S. 2022. Clathrin-independent endocytic retrieval of SV proteins mediated by the clathrin adaptor AP-2 at mammalian central synapses. eLife 11, e71198.

Macia E, Ehrlich M, Massol R, Boucrot E, Brunner C, Kirchhausen T. 2006. Dynasore, a cell-permeable inhibitor of dynamin. Dev Cell 10, 839-850.

Mahapatra S, Fan F, Lou X. 2016. Tissue-specific dynamin-1 deletion at the calyx of

Held decreases short-term depression through a mechanism distinct from vesicle resupply. Proc Natl Acad USA, E3150-3158.

Mahapatra S. & Lou X. 2017. Dynamin-1 deletion enhances post-tetanic potentiation and quantal size after tetanic stimulation at the calyx of Held. J Physiol 595, 193-206.

Marie B, Sweeney, Poskanzer KE, Roos J, Kelly RB, Davis GW. 2004. Dap160/Intersectin Scaffolds the periactive zone to achieve high-fidelity endocytosis and normal synaptic growth. Neuron 43, 207-219.

Miki T, Malagon G, Pulido C, Lliano I, Neher E, Marty A. 2016. Actin- and myosin-dependent vesicle loading of presynaptic docking sites prior to exocytosis. Neuron 91, 808-823.

Neher E, Sakaba T. 2008. Multiple roles of calcium ions in the regulation of neurotransmitter release. Neuron 25, 861-872.

Newton AJ, Kirchhausen T, Murthy VN. 2006. Inhibition of dynamin completely blocks compensatory synaptic vesicle endocytosis. Proc Natl Acad Sci USA 103, 17955-17960.

Park D, Lee U, Cho E, Zhao H, Kim JA, Lee BJ, Regan P, Ho W-K, Cho K, Chang S. 2018. Impairment of release site clearance within the active zone by reduced SCAMP5 expression causes short-term depression of synaptic release. Cell Rep 22, 3339-3350.

Park RJ, Shen H, Liu L, Liu X, Ferguson SM, De Camilli P. 2013. Dynamin triple knockout cells reveal off target effects of commonly used dynamin inhibitors. J Cell Sci 126, 5305-5312.

Rajappa R, Gauthier-Kemper A, Boning D, Huve J, Klingauf J. 2016. Synaptophysin 1 clears synaptobrevin 2 from the presynaptic active zone to prevent short-term

depression. Cell Rep 14, 1369-1381.

Renden R, von Gesdorff H. 2007. Synaptic vesicle endocytosis at a CNS nerve terminal: Faster kinetics at physiological temperatures and increased endocytic capacity. J Neuorphysiol 98, 3349-3359.

Sakaba T, Knonenko NL, Bacetic J, Pechstein A, Schmoranzer J, Yao L, Barth H, Schupliakov O, Kobler O, Aktories K, Haucke V. 2013. Fast neurotransmitter release regulated by the endocytic scaffold intersectin. Proc Natl Acad Sci USA 110, 8266-8271.

Sanchez-Alavez M, Alboni S, Conti B. 2011. Sex- and age-specific differences in core body temperature of c57Bl/6 mice. Age (Dordr) 33, 89-99.

Silver IA, Erecinska M. 1990. Intracellular and extracellular changes of [Ca^{2+}] in hypoxia and ischemia in rat brain in vitro. J gen Physiol 95, 837-866.

Sonntag, M., Englitz, B., Kopp-Scheinpflug, C., and Rubsamen, R. 2009. Early postnatal development of spontaneous and acoustically evoked discharge activity of principal cells of the medial nucleus of the trapezoid body: an in vivo study in mice. J Neurosci 29, 9510-9520.

Sun J-Y, Wu X-S, Wu W, Jin S-X, Dondzillo A, Wu L-G. 2004. Capacitance measurements at the calyx of Held in the medial nucleus of the trapezoid body. J Neurosci Met 134, 121-131.

von Kleist L, Stahlschmidt W, Bulut H, Gronova K, Puchkov D, Robertson MJ, MacGregor KA, Tomilin N, Chau N, Chircop M, Sakoff J, von Kries JP, Saenger W, Krausslich H-G, Schpuliakov O, Robinson PJ, McCluskey A, Haucke W . 2011. Cell 146, 471-484.

Wang L-Y, Kaczmarek LK. 1998. High-frequency firing helps replenish the readily

releasable pool of synaptic vesicles. Nature 394, 384-388.

Watanabe S, Rost BR, Camacho-Perez M, Davis MW, Shohl-Kielczynski B, Rosemund C, Jorgensen EM. 2013. Ultrafast endocytosis at mouse hippocampal synapses. Nature 504, 242-247.

Willox AK, Sahraoui YME, Royle SJ. 2014. Non-specificity of Pitstop 2 in clathrin-mediated endocytosis. Biol Open 3, 326-331.

Wu W, Xu J, Wu XS, Wu LG. 2005. Activity-dependent acceleration of endocytosis at a central synapse. J Neurosci 25, 11676-11683.

Yamashita T, Eguchi K, Saitoh N, von Gersdorff H, Takahashi T. 2010. Developmental shift to a mechanism of synaptic vesicle endocytosis requiring nanodomain Ca^{2+}. Nat. Neurosci.13, 838-844.

Yamashita T, Hige T, Takahashi T. 2005. Vesicle endocytosis requires dynamin-dependent GTP hydrolysis at a fast CNS syapse. Science. 307, 124-127

Yamashita T, Kanda T, Eguchi K, Takahashi T. 2009. Vesicular glutamate filling and AMPA receptor occupancy at the calyx of Held synapse of immature rats. J Physiol 587, 2327-2339.

Yu Y, Chu P-Y, Bowser DN, Keating DJ, Dubach D, Harper I, Tkalcevic J, Finkelstein DI, Pritchard MA. 2008. Mice deficient for the chromosome 21 ortholog *Itsn* 1exhibit vesicle-trafficking abnormalities. Hum Molec Genet 17, 3281-3290.

Figure title and legends:

Figure 1. The endocytic blocker Dynasore or Pitstop-2 inhibits slow, fast-accelerating and fast endocytosis at the calyx of Held

(A) Average traces of slow endocytic membrane capacitance changes (ΔC_m) in response to a 5-ms depolarizing pulse (stepping from -70 mV to +10 mV) in the absence (control, black trace) or presence of Dynasore (100 µM, 10-60 min, brown trace) or Pitstop-2 (25 µM, 10-60 min, green trace), recorded from the calyx of Held presynaptic terminal in slices from P13-15 mice at physiological temperature (PT, 37°C) and in 2.0 mM Ca^{2+} aCSF. The 4th panel from the left shows the superimposed average ΔC_m traces under control, Dynasore and Pitstop-2. The rightmost bar graph shows the endocytic decay rate (calculated from the slope 0.45-5.45 s after stimulation) that was slower in the presence of Dynasore (8.5 ± 2.8 fF/s; n = 5; p = 0.004, Student's t-test) or Pitstop-2 (11.9 ± 3.4 fF/s; n = 5; p = 0.015) than control (28.8 ± 3.7 fF/s; n = 5). Significance level was set at $p < 0.05$, denoted with asterisks (*$p < 0.05$, **$p < 0.01$, ***$p < 0.001$)

(B) Fast-accelerating endocytosis induced by a train of 20-ms depolarizing pulses (repeated 15 times at 1 Hz) in the absence (control) or presence of Dynasore or Pitstop-2. Averaged traces are shown as in (A). The 4th panel shows the endocytic rates (fF/s) calculated from the slope of C_m decay, 0.45-0.95 ms after each stimulation pulse under control, Dynasore, or Pitstop-2 (superimposed). The rightmost bar graph shows the endocytic rate averaged from stimulations #12-15 (bar in 4th panel) that was slower in the presence of Dynasore (121 ± 19 fF/s, n = 6; p = 0.0045, Student's t-test) or Pitstop-2 (133 ± 16 fF/s, n = 5; p = 0.007) than control (251 ± 28 fF/s; n = 6), indicating significant inhibition of the fast-accelerating endocytosis by Dynasore or Pitstop-2 (also see Table S1).

(C) Fast-endocytosis (average traces) evoked by a train of 20-ms pulses (repeated 10 times at 10 Hz) in the absence (control) or presence of Dynasore or Pitstop-2. The 4th panel shows cumulative ΔC_m traces (superimposed) in an expanded timescale during and immediately after the 10-Hz train. The rightmost bar graph indicates endocytic decay rates (measured 0.45-1.45 s after the 10th stimulation) in Dynasore (204 ± 25.3 fF; n = 4; p = 0.02; Student's t-test) or in Pitstop-2 (131 ± 24.6 fF; n = 4; p = 0.002) both of which were significantly slower than control (346 ± 40.1 fF; n = 6).

Figure 2. Endocytic blockers rapidly enhance synaptic depression in a stimulation frequency-dependent manner, but do not prolong the recovery from depression at the calyx.

(A1, B1) A train of 30 EPSCs were evoked at the calyx of Held by afferent fiber

stimulation at 10 Hz (A1) or 100 Hz (B1) in the absence (control, black traces) or presence of Dynasore (10-60 min, brown traces) or Pitstop-2 (10-60 min, green traces) at PT (37°C) in 1.3 mM Ca^{2+} aCSF. *Panels from left to right:* left-top: sample EPSC traces; left-bottom: normalized average EPSC amplitudes at each stimulus number; right-top bar graph: steady-state depression of EPSC amplitudes (mean of EPSCs #26-30, bar in the second panel); right-bottom: 1st-3rd EPSC amplitudes in expanded timescale.

(A2, B2) The recovery of EPSCs from STD in control, or in the presence of Dynasore or Pitstop-2 at the calyx of Held measured using a stimulation protocol (shown on top in A2); a train of 30 stimulations at 10 Hz (A2) or 100 Hz (B2) followed by test pulses after different time intervals (Δt: 0.02, 0.1, 0.3, 1, 3, 8, 12, and 20s). The EPSC amplitude after Δt ($I_{\Delta t}$) relative to the first EPSC in the stimulus train (I_{1st}) was normalized by subtracting the steady state EPSCs (I_{ss}) to measure the recovery rates.

(A1) During 10-Hz stimulation, the steady-state depression under control (0.55 ± 0.02; n = 11) was slightly enhanced in the presence of Dynasore (0.48 ± 0.02; n = 12; p = 0.03, Student's t-test) but not in Pitstop-2 (0.53 ± 0.02; n = 7; p = 0.4, no significant difference).

(A2) After 10-Hz stimulation, the time constant of EPSCs recovery in control (2.3 ± 0.4 s; n = 9) was unchanged in the presence of either Dynasore (1.7 ± 0.2 s; n = 8; p = 0.2, Student's t-test) or Pitstop-2 (1.9 ± 0.3 s; n = 7; p = 0.4).

(B1) During 100-Hz stimulation, EPSCs underwent a significant depression starting at the 2nd stimulation (10 ms) in Dynasore (0.6 ± 0.03; n =10; $p < 0.001$, t-test) or Pitstop-2 (0.65 ± 0.06; n = 7; p = 0.005) than control (0.91 ± 0.05; n = 11). Bar graph indicates STD magnitudes; control: (0.42 ± 0.025), Dynasore: (0.25 ± 0.02; $p < 0.001$), and Pitstop-2: (0.26 ± 0.03; $p < 0.001$).

(B2) After 100-Hz stimulation, both fast and slow recovery time constants were significantly faster in the presence of Dynasore or Pitstop-2 than control (bar graphs, Table S2).

Figure 3. Scaffold machinery inhibitors have no effect on endocytic membrane retrievals at the calyx of Held

The CDC42 inhibitor ML141 (10 μM, 10-60 min, cyan) or actin depolymerizer Latrunculin B (Lat-B, 10-60 min, 15 μM, red) had no effect on slow endocytosis in response to a 5-ms depolarizing pulse (A) or on fast accelerating endocytosis (B;

induced by 1-Hz train of 20 ms x 15 pulses) or fast endocytosis (C; evoked by a 10-Hz train of 20 ms x 10 pulses) at PT and in 2.0 mM Ca^{2+} aCSF.

(A) Averaged and superimposed ΔC_m traces in response to a 5-ms pulse. The rightmost bar graph indicates the endocytic decay rate in control (28.8 ± 3.7 fF; n = 5), unchanged by ML141 (21.9 ± 5.8 fF; n = 6; p = 0.42, Student's t-test) or Lat-B (28.5 ± 5.2 fF; n = 6; p = 0.97, Table S1).

(B) The average endocytic rate (#12-15) in control (251 ± 28 fF/s; n = 6) unaltered by ML141 (214 ± 19 fF/s; n = 5; p = 0.3, Student's t-test) or Latrunculin-B (233 ± 48 fF/s; n = 4; p = 0.7; Table S1).

(C) Fast endocytic decay rate in the presence of ML141 (242 ± 21.5 fF; n = 4; p = 0.054, t-test) or Lat-B (350 ± 33.3 fF; n = 5; p = 0.95) was not different from control (346 ± 40.1 fF; n = 6; Table S1).

Figure 4. Scaffold machinery inhibitors strongly enhance synaptic depression in a stimulation frequency-independent manner, without prolonging the recovery from depression at the calyx

(A1, B1) EPSCs (30x) evoked at the calyx of Held by afferent fiber stimulation at 10 Hz (A1) or 100 Hz (B1) in the absence (control, black) or presence of ML141 (10-60 min, cyan) or Lat-B (10-60 min, red) at PT and in 1.3 mM Ca^{2+} aCSF. *Panels from left to right:* like Figure 2.

(A2, B2) The recovery of EPSCs from STD in control, or in the presence of ML141 or Latrunculin-B at the calyx of Held measured at 10 Hz (A2) or 100 Hz (B2) – like figure 2.

(A1) At 10-Hz stimulation, enhancement of depression became significant from the 3rd stimulation (200 ms) in the presence of ML141 (0.61 ± 0.03; n = 9; p = 0.013, Student's t-test) or Lat-B (0.55 ± 0.04; n = 7; p = 0.006) compared to control (0.74 ± 0.04, n = 11). Bar graph indicates the steady-state depression (STD) strongly enhanced from control (0.55 ± 0.02) by ML141 (0.4 ± 0.02; p < 0.001) or Lat-B: (0.36 ± 0.02; p < 0.001).

(A2) After a train of 30 stimulations at 10 Hz, the time constant of EPSCs recovery under control was unchanged by ML141 or Latrunculin-B (Table S2).

(B1) At 100-Hz stimulation, EPSCs showed significant enhancement of depression at the 2nd stimulation (10 ms) in the presence of ML141 (0.65 ± 0.05; n = 10; p < 0.001) or Lat-B (0.58 ± 0.05; n = 8; p < 0.001) from control (0.91 ± 0.05; n = 11). Bar graph indicates strong STD produced by ML141 (0.22 ± 0.02; p < 0.001) or

Lat-B (0.18 ± 0.013; $p < 0.001$) compared to control (0.42 ± 0.025).

(B2) The time course of EPSC recovery from STD induced by a train of 30 stimulations at 100 Hz, indicating no significant change caused by ML141 or Lat-B in the recovery time constants (Table S2). The stimulation and recovery protocols were the same as those used in Figure 2.

Figure 5. Endocytic and scaffold machineries co-operate for rapid vesicle replenishment during high-frequency transmission at the calyx of Held.

(A) Exponential curve fits to the time-course of synaptic depression during 100-Hz stimulation under control and in the presence of either endocytic blockers or scaffold cascade inhibitors. The control time-course was best fit to a single exponential, whereas the time-course in the presence of endocytic blockers or scaffold cascade blockers was fit best to double exponential function with fast and slow time constants.

(B) Parameters for the curve-fit, including fast and slow time constants (τ_{fast}, τ_{slow}), weighted mean time constant (τ_{mean}) and relative ratio of fast and slow components (A_f/A_s). Similar fast time constant (τ_{fast}) in the presence of endocytic inhibitors or scaffold cascade inhibitors suggests simultaneous operation of endocytic and scaffold mechanisms for countering the synaptic depression. Similar slow decay time constant irrespective of the presence or absence of blockers suggests that the endocytosis and scaffold mechanisms for vesicle replenishment operates predominantly at the beginning of the high frequency stimulations.

(C) Enhancement of synaptic depression by co-application of Dynasore and Latrunculin-B (10-60 min) was like Latrunculin-B alone and stronger than Dynasore alone. Sample EPSC traces and normalized depression time courses are shown on the upper and lower left panels, respectively. The STD magnitudes are compared in bar graph; control: (0.42 ± 0.025; n = 11), Dynasore: (0.25 ± 0.02; n = 10, $p = 0.009$), Latrunculin-B: (0.18 ± 0.013; n = 8, $p = 0.005$ vs Dynasore), and Dyn + Lat-B together: (0.17 ± 0.02; n = 11; $p = 0.005$ vs Dynasore).

Figure 6. Endocytic blockers attenuate synaptic facilitation, but scaffold cascade inhibitors have no effect at hippocampal CA1 synapses

(A-D) A train of 30 EPSCs evoked in hippocampal CA1 pyramidal cells by Schaffer

collateral stimulation at 10 Hz (A and C) or 25 Hz (B and D) in the absence (control, black) or presence of endocytic blocker Dynasore (100 μM, 10-60 min, brown) or Pitstop-2 (25 μM, 10-60 min, green) (A, B), or scaffold protein inhibitor ML141 (10 μM, 10-60 min, cyan) or Latrunculin-B (15 μM, 10-60 min, red) (C, D) at PT (37°C) and in 1.3 mM Ca^{2+} aCSF. Top panels show sample EPSC traces. Lower panels show average EPSC amplitudes normalized and plotted against stimulation numbers. Bar graphs show EPSCs amplitudes averaged from #26-30 events.

(A) At 10 Hz stimulation, EPSCs in control showed facilitation reaching a peak at the 7th stimulation (2.34 ± 0.3; n = 17). At this point, in the presence of Dynasore (1.44 ± 0.15; n = 10; p = 0.012, Student's t-test) facilitation was significantly attenuated. The effect of Pitstop-2 (1.85 ± 0.14; n = 14; p = 0.06) was not different. Towards the end of stimulus train (#26-30), synaptic facilitation in control (1.85 ± 0.17) was significantly attenuated by Dynasore (0.83 ± 0.07; p < 0.001) or Pitstop-2 (1.21 ± 0.08; p = 0.002).

(B) At 100 Hz stimulation, synaptic facilitation peaked at the 12th stimulation in control (3.5 ± 0.4; n = 16), at which the facilitation was significantly attenuated by Dynasore (1.6 ± 0.11; n = 11; p < 0.001, t-test) or Pitstop-2 (2.11 ± 0.22; n = 14; p = 0.004). Also, at #26-30, synaptic facilitation in control (2.65 ± 0.3) was strongly attenuated by Dynasore (0.94 ± 0.1; p < 0.001) or Pitstop-2 (1.62 ± 0.2; p = 0.006).

(C) At 10 Hz stimulation, the peak facilitation at the 7th stimulation in control (2.34 ± 0.3; n = 17) was not significantly changed by ML141 (2.5 ± .22, n = 10; n = 0.75, Student's t-test) or Lat-B (2.3 ± 0.23; n = 12; p = 0.93). Likewise, the facilitation at #26-30 in control (1.85 ± 0.17) was not altered by ML141 (2.03 ± 0.16; p = 0.44) or Lat-B (1.84 ± 0.1; p = 0.96).

(D) At 100 Hz stimulation, peak facilitation at 12th stimulation in control (3.5 ± 0.4; n = 16) was unchanged by ML141 (3.3 ± 0.34; n = 10; p = 0.72, t-test) or Lat-B (3.1 ± 0.4; n = 11; p = 0.42). Facilitation at #26-30 events in control (2.65 ± 0.3) was also unaltered by ML141 (2.53 ± 0.2; p = 0.74) or Lat-B (2.5 ± 0.25; p = 0.7).

Figure 7. Hypothetical vesicle replenishment scheme by endocytosis and scaffold-machineries during repetitive transmission at fast-signaling calyx and slow-plastic hippocampal CA1 synapses.

During high-frequency transmission, endocytosis driven site-clearance allows activity-dependent replenishment of new vesicles to release sites. This endocytic function counteracts synaptic depression caused by vesicle depletion, thereby maintain synaptic strength, enabling high-fidelity fast neurotransmission at sensory relay synapses, like at

the calyx of Held. This endocytosis driven synaptic strengthening function augments synaptic facilitation at slow-plastic synapses like hippocampal CA1 synapses that exhibit long-term plasticity, thereby boosting its induction capability for memory formation. Whereas, the presynaptic scaffold machinery plays a powerful direct vesicle replenishment role, independent of endocytosis and activity, thereby rapidly translocating new vesicles to open release sites including those just opened by endocytic site-clearance. This scaffold function is specifically devoted to fast-signaling synapses, with high release probability but not to plastic synapses, where vesicle depletion is minimal due to low release probability.

Figure 1

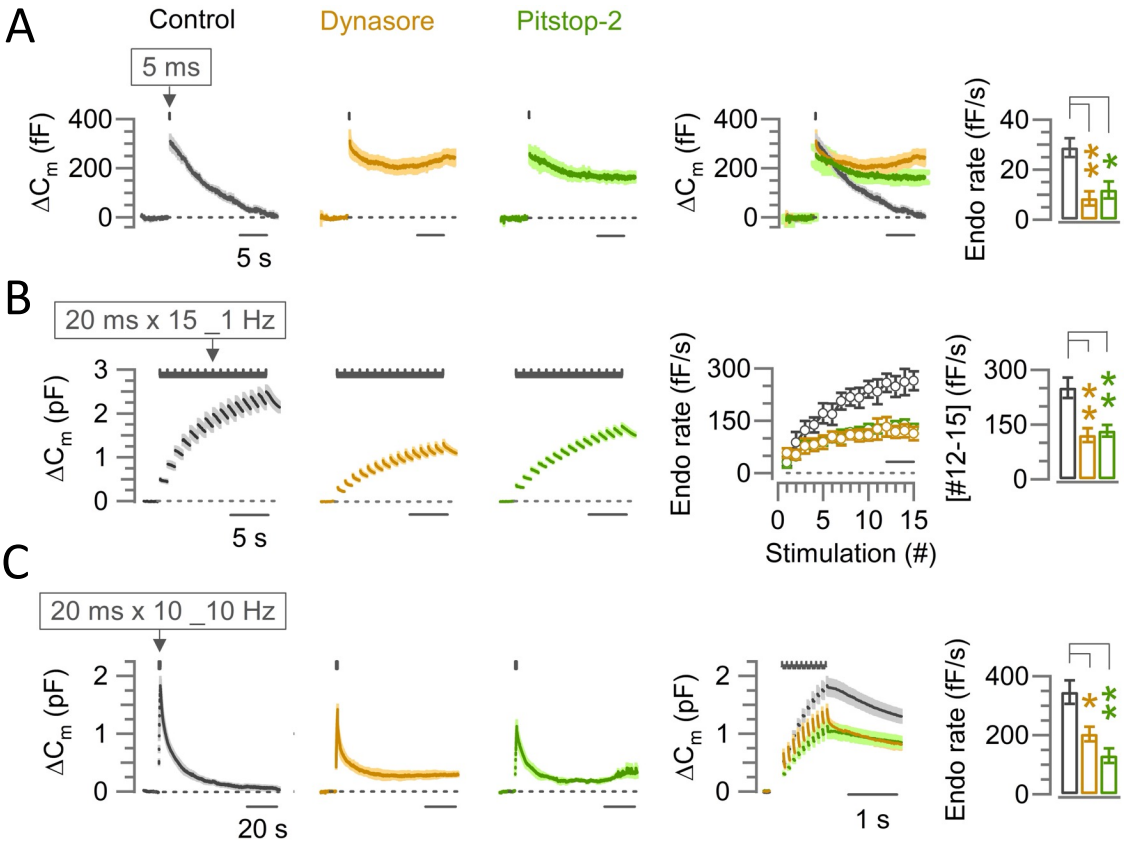
A
Control
Dynasore
Pitstop-2
5 ms
ΔCm (fF)
400
200
0
5 s
Endo rate (fF/s)
40
20
0
B
20 ms x 15 _1 Hz
ΔCm (pF)
3
2
1
0
5 s
Endo rate (fF/s)
300
150
0
0 5 10 15
Stimulation (#)
[#12-15] (fF/s)
C
20 ms x 10 _10 Hz
20 s
1 s

Figure 2

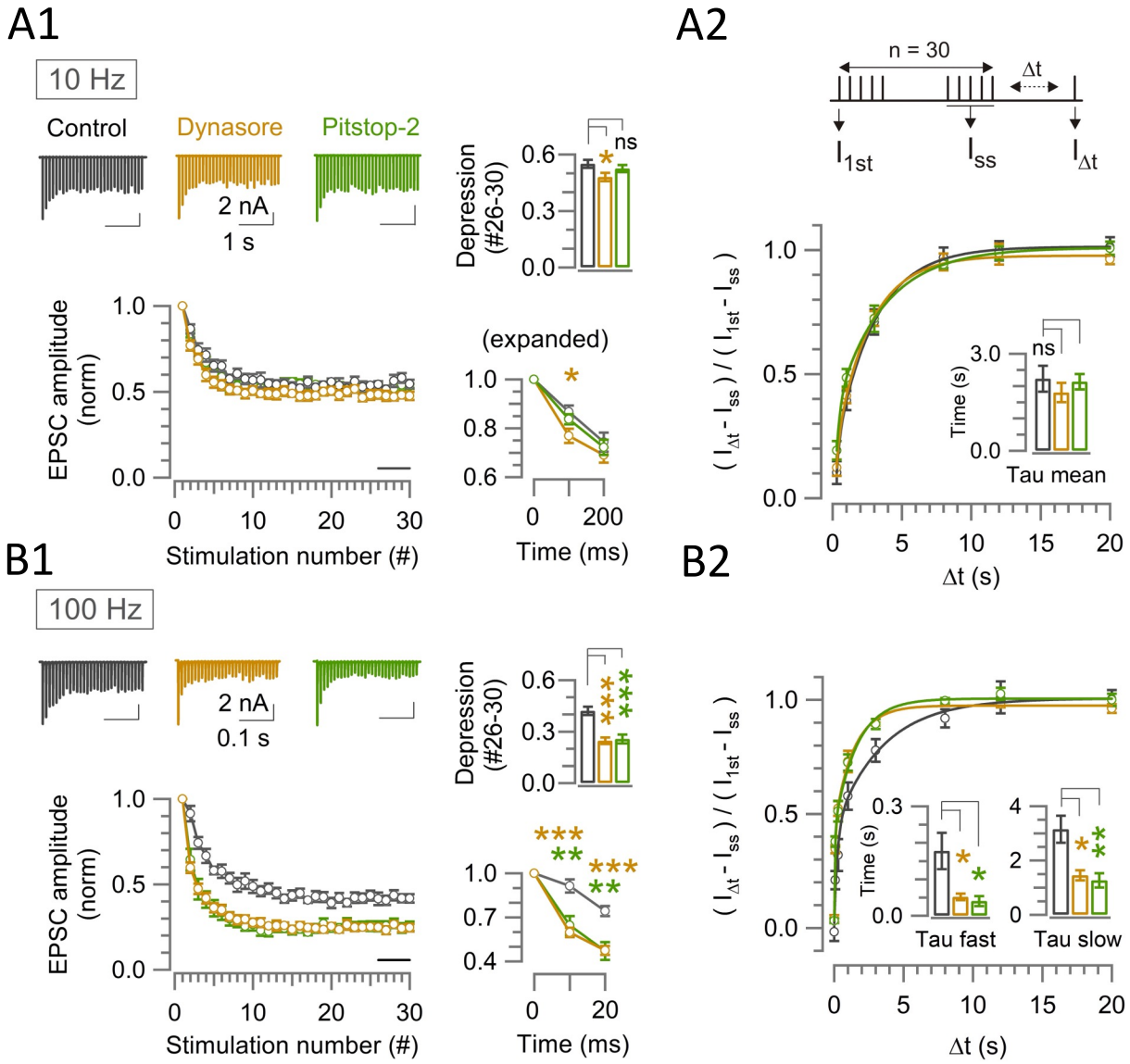
A1
10 Hz
Control
Dynasore
Pitstop-2
2 nA
1 s
EPSC amplitude (norm)
Stimulation number (#)
Depression (#26-30)
ns
(expanded)
Time (ms)
A2
n = 30
Δt
I1st
Iss
IΔt
(IΔt - Iss) / (I1st - Iss)
Time (s)
Tau mean
B1
100 Hz
2 nA
0.1 s
B2
Tau fast
Tau slow

Figure 3

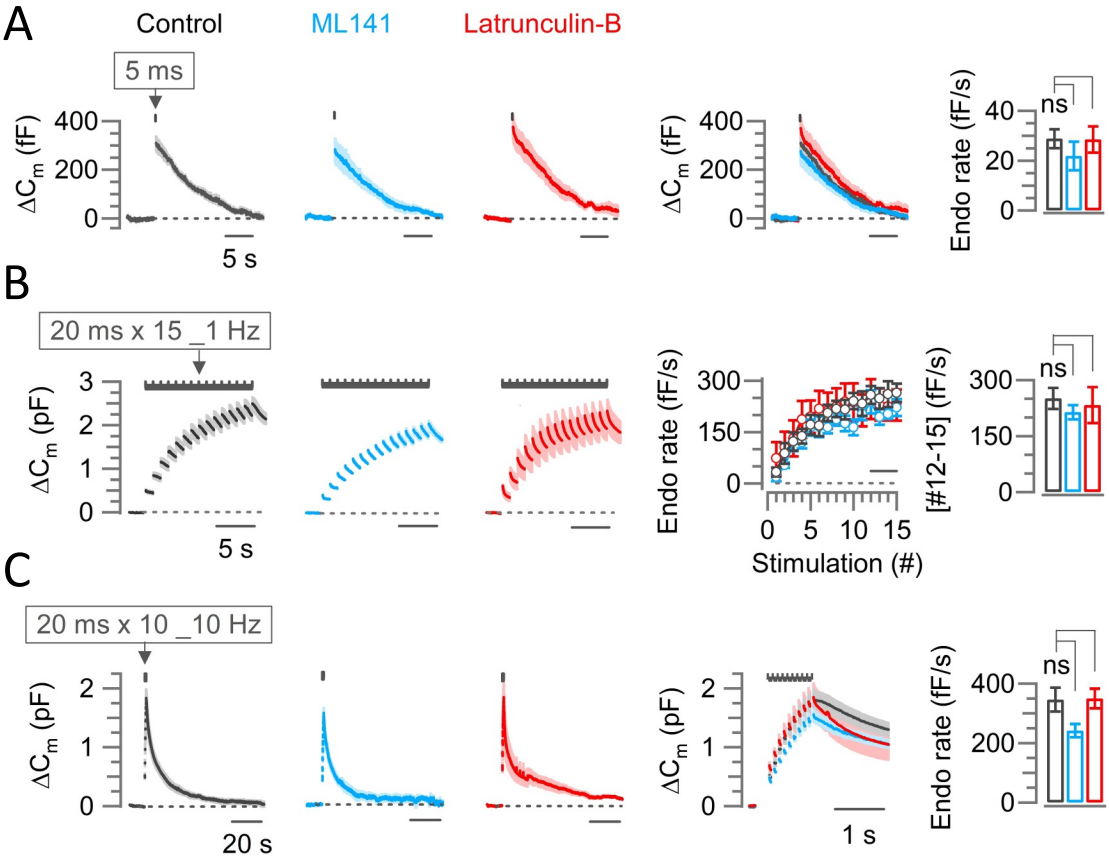
A
Control
ML141
Latrunculin-B
5 ms
ΔCm (fF)
400
200
0
5 s
Endo rate (fF/s)
40
20
ns
B
20 ms x 15 _1 Hz
ΔCm (pF)
3
2
1
Endo rate (fF/s)
300
150
0 5 10 15
Stimulation (#)
[#12-15] (fF/s)
C
20 ms x 10 _10 Hz
20 s
1 s

Figure 4

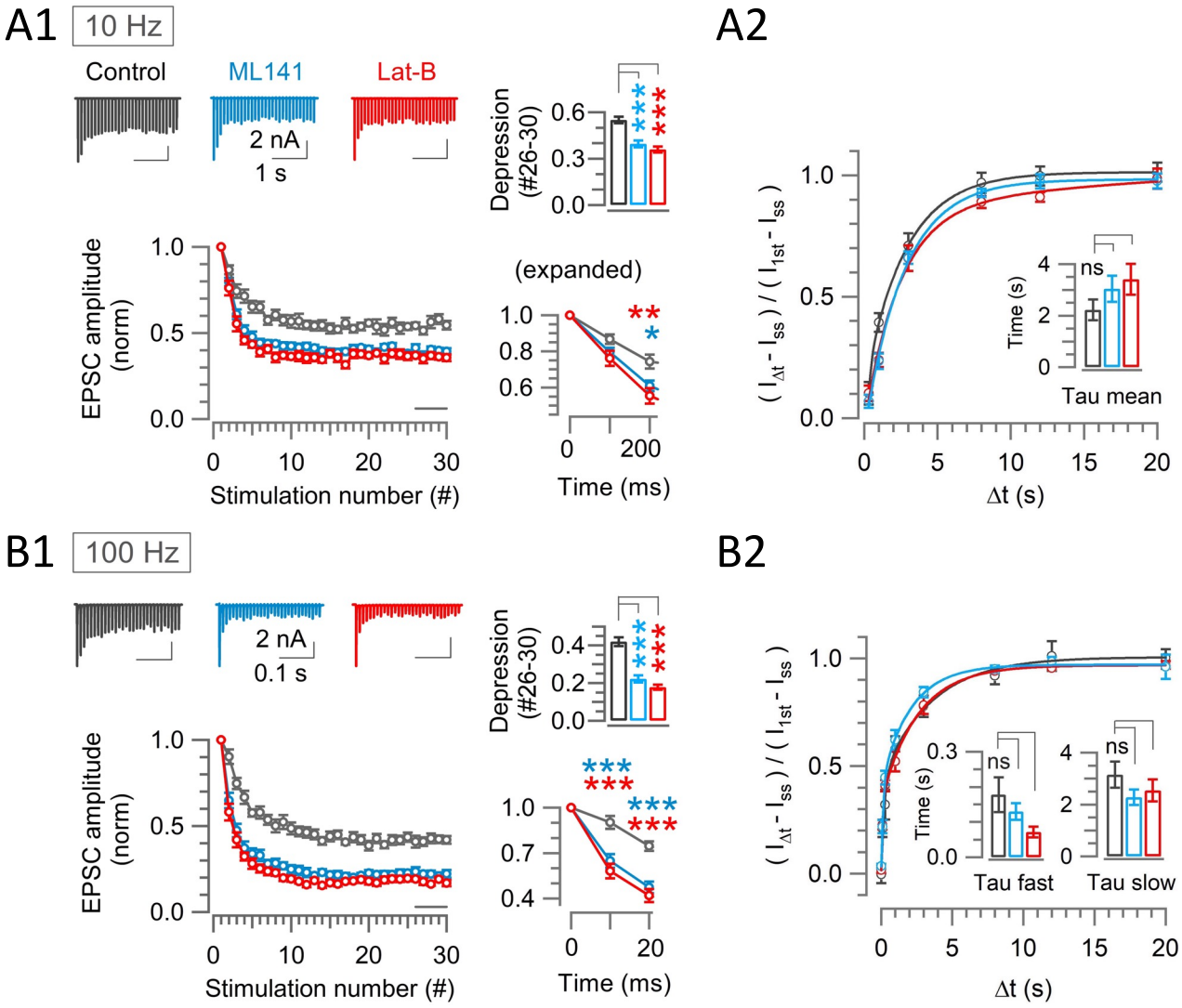
A1
10 Hz
Control
ML141
Lat-B
2 nA
1 s
Depression (#26-30)
0.6
0.3
0.0
EPSC amplitude (norm)
1.0
0.5
0.0
0
10
20
30
Stimulation number (#)
(expanded)
1.0
0.8
0.6
0
200
Time (ms)
A2
(I_Δt - I_ss) / (I_1st - I_ss)
1.0
0.5
0.0
0
5
10
15
20
Δt (s)
Time (s)
4
2
0
ns
Tau mean
B1
100 Hz
2 nA
0.1 s
Depression (#26-30)
0.4
0.2
0.0
EPSC amplitude (norm)
1.0
0.5
0.0
0
10
20
30
Stimulation number (#)
1.0
0.7
0.4
0
20
Time (ms)
B2
(I_Δt - I_ss) / (I_1st - I_ss)
1.0
0.5
0.0
0
5
10
15
20
Δt (s)
Time (s)
0.3
0.0
ns
Tau fast
4
2
0
ns
Tau slow

Figure 5

A

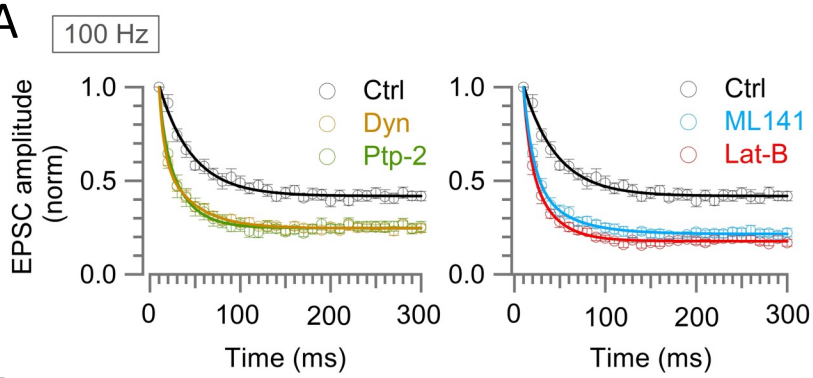

B

100 Hz	τ_{fast}	τ_{slow}	τ_{mean}	A_f/A_s
Ctrl	-	-	37 ms	-
Dyn Ptp-2	5 ms 6 ms	35 ms 24 ms	11 ms 13 ms	0.90 0.44
ML141 Lat-B	10 ms 7 ms	40 ms 26 ms	18 ms 13 ms	3.1 2.2

C

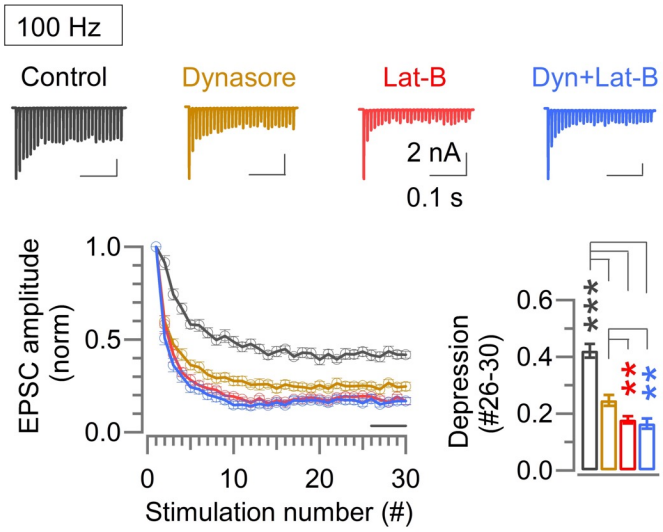

Figure 6

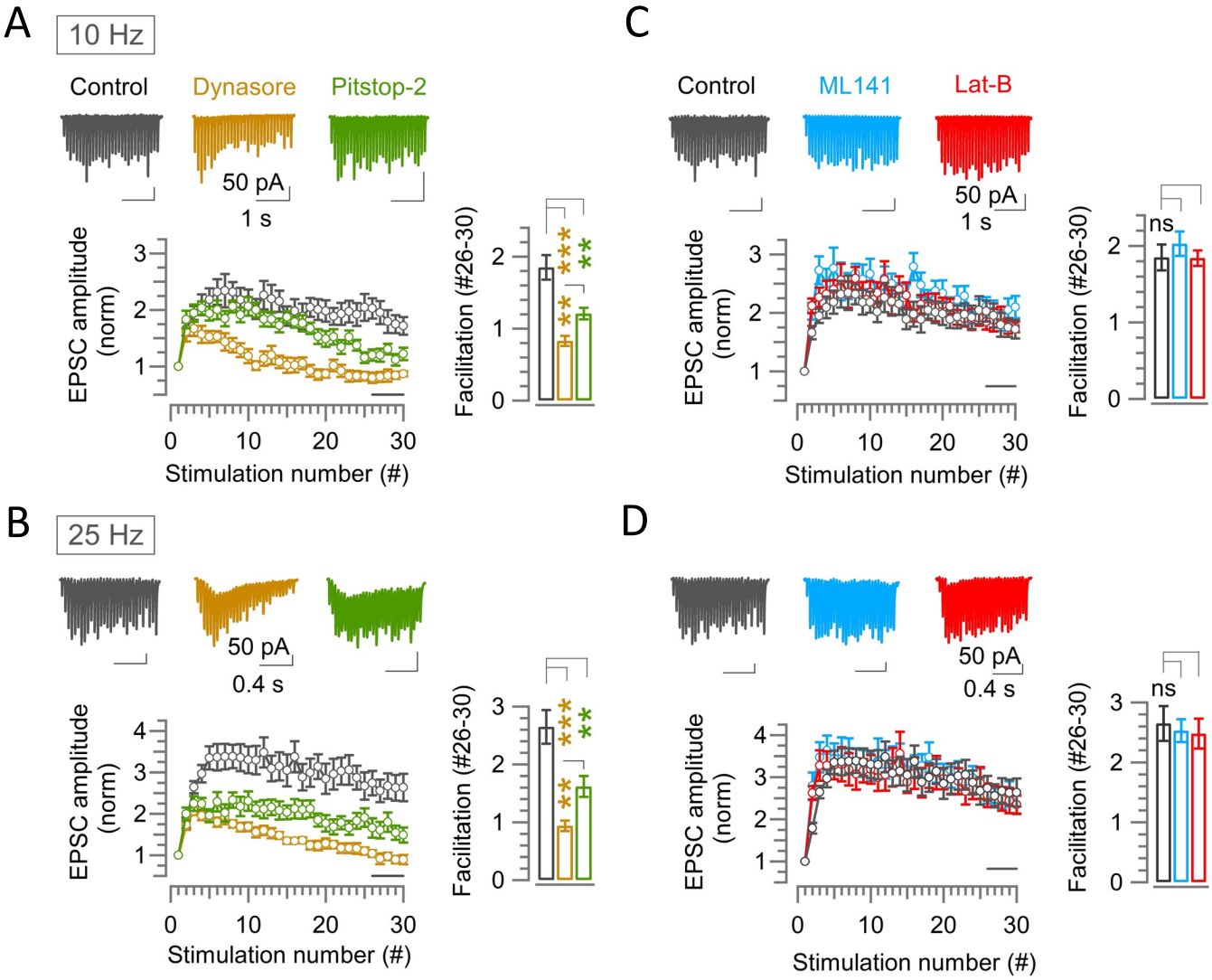
A
10 Hz
Control
Dynasore
Pitstop-2
50 pA
1 s
EPSC amplitude (norm)
Stimulation number (#)
Facilitation (#26-30)
B
25 Hz
50 pA
0.4 s
C
Control
ML141
Lat-B
ns
D

Figure 7

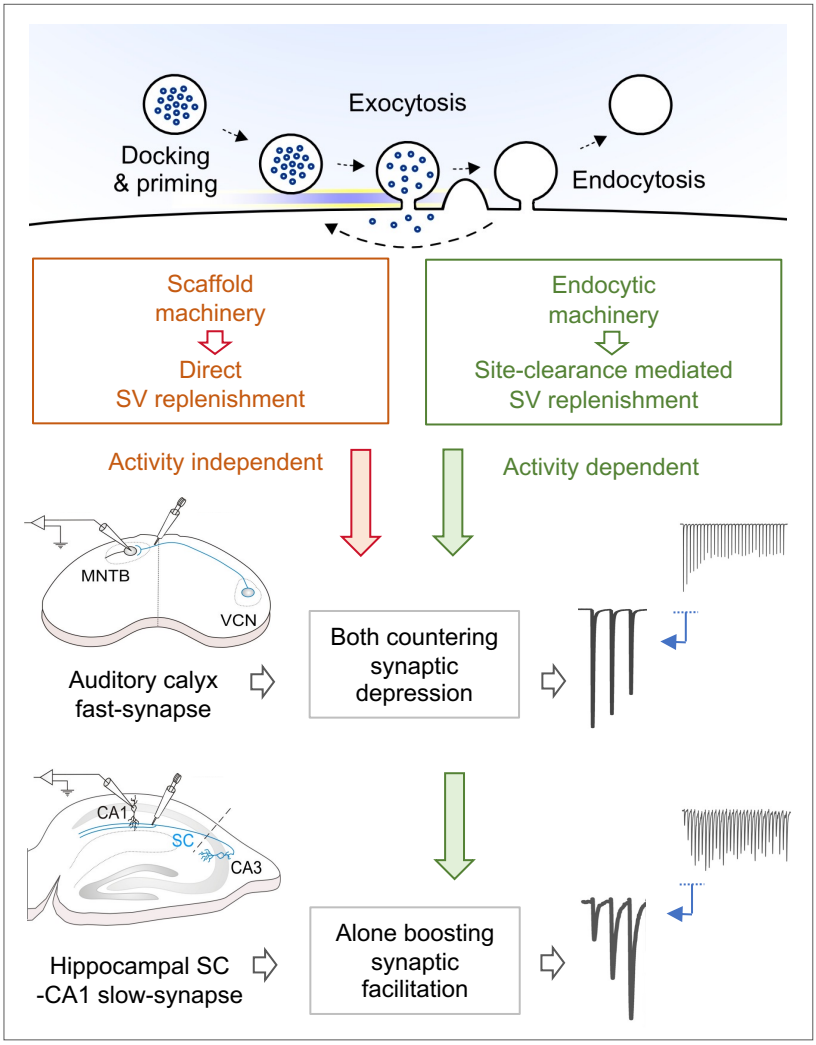
Exocytosis
Docking
& priming
Endocytosis
Scaffold
machinery
Direct
SV replenishment
Endocytic
machinery
Site-clearance mediated
SV replenishment
Activity independent
Activity dependent
MNTB
VCN
Auditory calyx
fast-synapse
Both countering
synaptic
depression
CA1
SC
CA3
Hippocampal SC
-CA1 slow-synapse
Alone boosting
synaptic
facilitation